# Geometric pre-patterning based tuning of the period doubling onset strain during thin film wrinkling

Sourabh K. Saha

Materials Engineering Division, Lawrence Livermore National Laboratory, PO Box 808, Livermore, California, 94550, USA

> February 16, 2017 Version 1.0

> LLNL-TR-724461





This document was prepared as an account of work sponsored by an agency of the United States government. Neither the United States government nor Lawrence Livermore National Security, LLC, nor any of their employees makes any warranty, expressed or implied, or assumes any legal liability or responsibility for the accuracy, completeness, or usefulness of any information, apparatus, product, or process disclosed, or represents that its use would not infringe privately owned rights. Reference herein to any specific commercial product, process, or service by trade name, trademark, manufacturer, or otherwise does not necessarily constitute or imply its endorsement, recommendation, or favoring by the United States government or Lawrence Livermore National Security, LLC. The views and opinions of authors expressed herein do not necessarily state or reflect those of the United States government or Lawrence Livermore National Security, LLC, and shall not be used for advertising or product endorsement purposes.

This work was performed under the auspices of the U.S. Department of Energy by Lawrence Livermore National Laboratory under Contract DE-AC52-07NA27344. The author utilized the postdoctoral funding for independent research available at LLNL to write this report. The author also thanks Prof. Martin Culpepper at MIT and Dr. Prakash Govindan at Gradiant Corporation for access to laboratory workspace for the experiments.

# Geometric pre-patterning based tuning of the period doubling onset strain during thin film wrinkling

Sourabh K. Saha\*

**Keywords:** buckling instability; higher modes; stretchable structures; bilayer wrinkling

#### **Abstract**

Wrinkling of supported thin films is an easy-to-implement and low-cost fabrication technique for generation of stretch-tunable periodic micro and nano-scale structures. However, the tunability of such structures is often limited by the emergence of an undesirable period doubled mode at high strains. Predictively tuning the onset strain for period doubling via existing techniques requires one to have extensive knowledge about the nonlinear pattern formation behavior. Herein, a geometric pre-patterning based technique is introduced to delay the onset of period doubling that can be implemented to predictively tune the onset strain even with limited system knowledge. The technique comprises pre-patterning the film/base bilayer with a sinusoidal pattern that has the same period as the natural wrinkle period of the system. The effectiveness of this technique has been verified via physical and computational experiments on the polydimethylsiloxane/glass bilayer system. It is observed that the period doubling onset strain can be increased from the typical value of 20% for flat films to greater than 30% with a modest pre-pattern aspect ratio (2:amplitude/period) of 0.15. In addition, finite element simulations reveal that (i) the onset strain can be increased up to a limit by increasing the amplitude of the pre-patterns and (ii) the delaying effect can be captured entirely by the pre-pattern geometry. As a result, one can implement this technique even with limited system knowledge, such as material properties or film thickness, by simply replicating pre-existing wrinkled patterns to generate prepatterned bilayers. Thus, geometric pre-patterning is a practical scheme to suppress period doubling that can increase the operating range of stretch-tunable wrinkle-based devices by at least 50%.

\_\_\_\_\_

\*Correspondence to: <a href="mailto:saha5@llnl.gov">saha5@llnl.gov</a>

# **Highlights**

- Geometric pre-patterning delays onset of period doubling during wrinkling
- Pre-patterning increases the deformation energy penalty for higher buckling modes
- Delaying effect is captured entirely by non-dimensional pre-pattern size
- Pre-patterning technique universally applicable even with limited system knowledge
- Wrinkles themselves can be used to generate the pre-patterns

#### 1 Introduction

The generation of wrinkled patterns via compression of supported thin films is a scalable and affordable technique for fabricating periodic micro and nano scale features over large areas [1-9]. The mechanism of wrinkle formation is similar to buckling of columns under compressive loads with one significant difference – the wrinkle period is independent of the in-plane length of the film. Instead, the wrinkle period depends only on the thickness of the film and the ratio of mechanical properties (Young's modulus and Poisson's ratio) of the film and base at the onset of buckling [10, 11]. Consequently, wrinkled patterns exhibit a distinct scale-independent "natural" period that can be well-controlled by tuning the film thickness and the elastic moduli ratio. In addition, the natural period and the amplitude of the wrinkles can be further tuned by controlling the magnitude of strain [12, 13]. Thus, well-controlled stretch-tunable periodic micro/nano scale patterns can be generated via wrinkling.

In the past, single-period sinusoidal wrinkles that were generated via uniaxial compression have been used as stretch-tunable functional features for applications such as tunable nano-fluidic channels [14, 15] and tunable diffraction gratings [16-18]. The degree of tunability of such devices is limited by the maximum strain that can be applied. Often, this maximum strain for tuning wrinkle patterns is limited by the onset of period doubling at high strains [13-19]. Period doubling refers to the emergence of an additional deformation mode in the wrinkle pattern wherein alternate valleys become progressively shallower with increasing strain. This behavior is illustrated in Fig. 1(a). Emergence of the period doubled mode leads to a complex pattern that is structurally, and often functionally, distinct from the initial single-period sinusoidal pattern. Thus, when a large design space for stretch-tunability is desired, one must suppress the onset of period doubling.

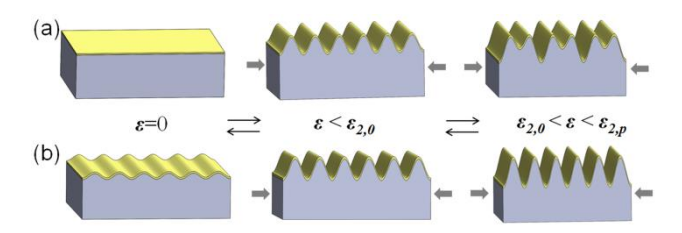


Fig. 1: Schematic representation of the formation and growth of wrinkles with strain during compression of (a) flat bilayers and (b) pre-patterned bilayers. Onset of period doubling is delayed in pre-patterned bilayers.

Although the phenomenon of period doubling at high compressive strains is well-known [13, 19-23], practical techniques to predictively and independently tune the onset strain are not available. Period doubling in wrinkling was first reported by Brau et al. [19] who empirically demonstrated the phenomenon and proposed an analytical model. Although their model predicts the amplitude of wrinkles post-doubling, their prediction that the onset strain is strongly dependent on only the Poisson's ratio of the base is impractical to implement. Since then, a more practical approach that is based on pre-stretching the base has been demonstrated to control the onset strain [22-24]. Although practical to implement, this pre-stretch based technique requires one to have extensive knowledge about the nonlinear mechanics of pattern formation to be able to predict the change in the onset strain. In addition, the degree of tunability of onset strain is coupled to and limited by the specific stress-strain constitutive relationship of the material. Herein, an alternate technique based on geometric pre-patterning is proposed that enables one to predict and determine the change in onset strain simply by knowing/selecting the size of the prepattern. Due to the universality of the first-order relationship between the non-dimensional prepattern size and the change in onset strain, this technique can be implemented to predictively tune the onset strain even when the material properties of the bilayer or the film thickness are unknown. Thus, this geometric pre-patterning technique enables one to predictively and independently tune the onset strain for a variety of bilayer wrinkling systems.

# 2 Geometric pre-patterning technique

The geometric pre-patterning technique for suppression of period doubling is illustrated in Fig. 1(b). Suppression of period doubling is achieved by pre-patterning the base layer with a sinusoidal pattern that has a period identical to the natural period of the equivalent flat bilayer system. The equivalent flat bilayer system is identical to the pre-patterned system except for the absence of geometric pre-patterning, i.e., the material properties, thin film thickness, and applied stretch in the flat and pre-patterned system are identical. The natural period of the equivalent flat bilayer system is the period of the wrinkles that emerge immediately at the onset of buckling. Upon compression of the pre-patterned bilayer, it is observed that the natural period persists at high strains and period doubling begins at a strain that is higher than that for the equivalent flat bilayer. As illustrated in Fig. 2, this behavior has been computationally and experimentally verified for the polydimethylsiloxane/glass bilayer system.

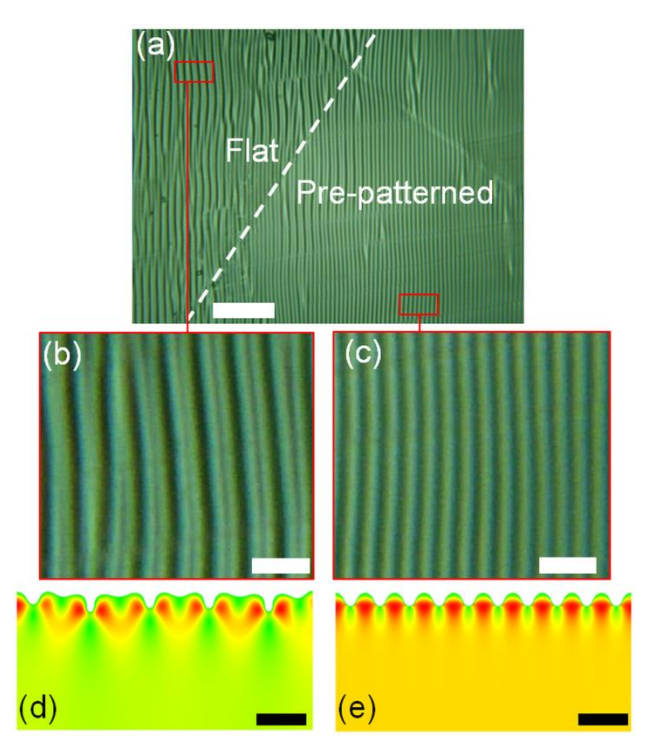


Fig. 2: Demonstration of delayed onset of period doubling via pre-patterning. (a) - (c) Fabricated wrinkles on top of flat and pre-patterned bilayer. Finite element modeling of wrinkles on (d) flat and (e) pre-patterned bilayer. The pre-pattern amplitude, strain, and natural period were [168 nm, 0.249, 2.0  $\mu$ m] for both experiments and simulations. Scale bars are 20  $\mu$ m long for (a) 5  $\mu$ m for (b) and (c) and 2.5  $\mu$ m for (d) and (e).

## 2.1 Physical demonstration

The experiments performed here separately identify the effect of pre-patterning on onset strain by decoupling it from the effect of material properties and strain. Distinct regions of period-doubled and single-period wrinkles were observed at the edge of the pre-patterned and flat sections of the same bilayer (Fig. 2). The pre-patterned region was fabricated by replicating a pre-existing wrinkled surface on top of polydimethylsiloxane (PDMS) during the curing process [25]. Wrinkled patterns were fabricated by (i) uniaxially stretching the PDMS base on a custom tensile stage[13], (ii) generating a thin glassy layer on top of the pre-stretched base by exposing it to air plasma [25, 26], and (iii) releasing the stretch in the base layer to generate uniaxial compressive strain in the glassy thin film. As the entire bilayer was subjected to the same stretch and was exposed to air plasma at once, the two regions differ only in the presence or absence of the pre-patterns.

#### 2.1.1 Fabrication technique

PDMS films were fabricated by casting and thermally curing a two-part polydimethylsiloxane (PDMS) silicone elastomer mix that is commercially available from Dow Corning (Sylgard 184). The two parts were mixed by combining 15 parts of resin and 1 part of curing agent by weight. A non-standard curing ratio of 15:1 was used because this combination was observed to generate PDMS films with the desirable mechanical properties of low Young's modulus and high failure stretch [27]. After degassing the mixture, curing was performed via a two-step thermal curing process so as to minimize the volumetric shrinkage in the film. Alignment features were generated on the bottom surface of the films by casting and curing the mixture in custom-made aluminum molds. These alignment features were later used to align the direction of stretch with the wrinkle pre-patterns. The Young's modulus of the cured PDMS was measured on an Instron tensile tester and found to be 1.893 ± 0.033 MPa [27].

The cured PDMS films were manually cut into individual coupons that were approximately 20 mm wide, 1.9-2.2 mm thick and had a clamped length of 37.5 mm. These coupons were then mounted and stretched on a custom-made precision tensile stage [13]. The accuracy of the clamped length was ensured by mating the alignment features on the coupons to the corresponding features on the stage. The entire stage with the stretched coupon was then inserted into a vacuum chamber and exposed to low-pressure RF air plasma. The air plasma chemically modifies the surface and generates a glassy thin film on top of the PDMS layer that has a measured Young's modulus of  $3.2 \pm 0.78$  GPa [27] and is 10-100 nm thick. The thickness of the glassy film can be tuned by controlling the duration of the plasma exposure. The plasma oxidation process was calibrated to link the observed period to the duration of exposure [27]. After plasma oxidation, wrinkles were generated by gradually releasing the stretch in the base layer thereby causing the top glassy layer to compress and buckle.

Pre-patterned regions on the film were fabricated by imprinting wrinkled surfaces onto the base during the thermal curing process. Imprinting was performed by gradually and "gently" placing the coupons with the wrinkled surfaces on top of the curing material after the onset of curing but before gelation. Alignment of the pre-patterns to the subsequent direction of stretch was achieved by visually sensing and then aligning the alignment marks on the coupons with the alignment marks on the mold. Post curing, the imprinted wrinkled patterns were carefully separated from the cured PDMS base to expose the pre-patterned region of the base. The

protocol for curing and imprinting is described in detail elsewhere [28]. As the oxidized glassy layer generated via plasma oxidation generates a thin film that is chemically bonded to the base PDMS, no delamination of the film was observed during detachment of the pre-pattern mold from the cured base film.

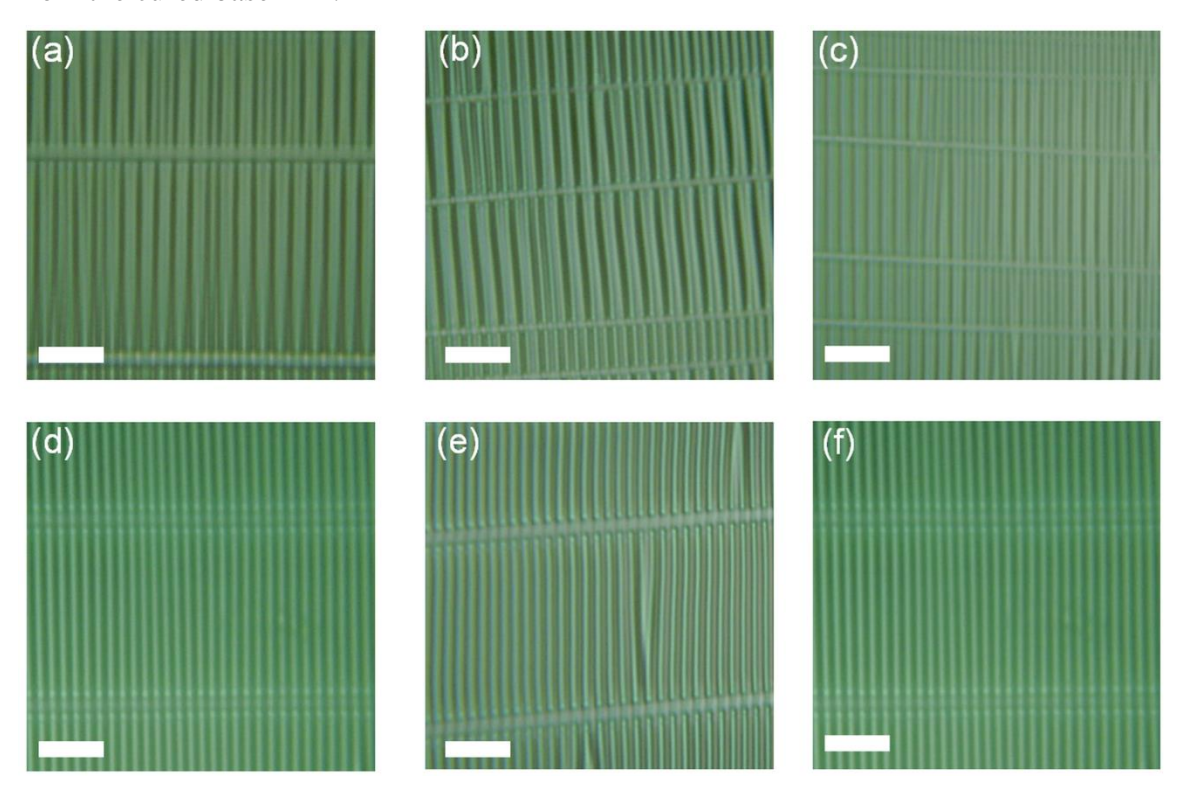


Fig. 3: Wrinkle patterns on three different bilayer samples, each with a pair of flat and prepatterned region. (a) - (c) period-doubled wrinkles on flat regions and (d) - (f) single-period wrinkles on the corresponding pre-patterned regions.  $\lambda_n$ ,  $\varepsilon_p$ , and  $\varepsilon$  for (a) and (d) were [2.3  $\mu$ m, 0.04, 0.255]; for (b) and (e) were [2.2  $\mu$ m, 0.07, 0.249]; for (c) and (f) were [2.3  $\mu$ m, 0.06, 0.245]. Scale bars are 10  $\mu$ m long.

#### 2.1.2 Demonstration of delayed doubling

Several experiments were performed to verify the delayed onset of period doubling by varying the pre-stretch in the base and the pre-pattern amplitude. The results of these experiments are summarized in Fig. 3. Wrinkles were fabricated on three different bilayer samples; each sample comprised a pair of flat and pre-patterned regions (pairs a-d, b-e, and c-f in Fig. 3). The flat and pre-patterned regions were fabricated on the same PDMS base to ensure that plasma oxidation and stretch were identical for the two regions. To ensure that both flat and pre-patterned regions were obtained on the same base: (i) the pre-pattern coupons were cut into

pieces that were each smaller than a single stretched PDMS coupon and (ii) during curing, only part of the PDMS base was imprinted with the pre-pattern to generate the pre-patterned region while the rest of the base surface was left untouched to generate the flat region. As illustrated in Fig. 3, period doubling was observed only on the flat regions of the sample (panels in top row of Fig. 3) but not on the pre-patterned regions of the same sample (panels in bottom row of Fig. 3). The natural period ( $\lambda_n$ ) was evaluated from the observed period in the images ( $\lambda_o$ ) and the applied strain ( $\varepsilon$ ) using an empirically verified approximation that the number of wrinkles does not change during compression as [13]:

$$\lambda_n = \lambda_o (1 + \varepsilon) \tag{1}$$

#### 2.2 Computational demonstration

#### 2.2.1 Finite element modeling technique

Finite element modeling was performed by developing 2-D models of wrinkling using the Structural Mechanics module of the COMSOL 5.1 software package and the MATLAB R2015a software package for pre and post-processing. These models were developed by implementing buckling of wide plates under the plane strain condition with the top film modeled as a linear elastic material and the bottom layer as a nonlinear Neo-Hookean material. A nonlinear strain-displacement relationship was used for both the layers to account for large angles during wrinkling. The bilayer was uniaxially compressed by simultaneously compressing the top and bottom layers. Modeling of wrinkle formation in flat bilayers was performed in two steps: (i) linear pre-buckling analysis to predict the mode shapes required for generating a perturbed mesh and (ii) a nonlinear post-buckling analysis on the perturbed mesh to predict the shape and amplitude of the wrinkles after buckling bifurcation. Modeling of wrinkle formation in prepatterned bilayers was performed on the perturbed mesh via a single-step nonlinear analysis. The perturbed mesh was generated from the pre-pattern geometry using a custom mesh-perturbation toolbox described in detail elsewhere [25, 31].

The boundary conditions for the finite element modeling of wrinkles are illustrated in Fig. 4(a). The height of the base layer was chosen to be sufficiently high (5  $\mu$ m) to simulate semi-infinite boundary condition at the lower edge. The length of the base layer was selected to be exactly 10 times the natural period so that no errors due to boundary discretization are introduced

during the simulation. This proportional base length condition was ensured by first evaluating the natural period via linear buckling analysis of a base of length 22.5  $\mu$ m and then re-generating a new model with base length 10 times the evaluated natural period.

#### 2.2.2 Demonstration of delayed doubling

The effect of pre-patterning on the period doubling onset strain is demonstrated in Fig. 4(b). The predictions of finite element simulations shown in Figs. 2 and 4 are consistent with the physically observed period doubling suppression behavior summarized in Fig. 2. During simulations, the onset strain was evaluated by tracking the growth of amplitude of the single-period and period-doubled modes as the film and base layers were compressed simultaneously. The applied strain ( $\varepsilon$ =0.249) for the fabricated pattern (Fig. 2) was higher than the predicted onset strain for the flat bilayer ( $\varepsilon_{2,0}$ =0.19) but less than the onset strain for the pre-patterned bilayer ( $\varepsilon_{2,p}$ =0.31). Thus, one expects to observe two distinct patterns at the pre-pattern/flat boundary with the single-period pattern lying on the pre-patterned side. This expected behavior was observed during the experiments.

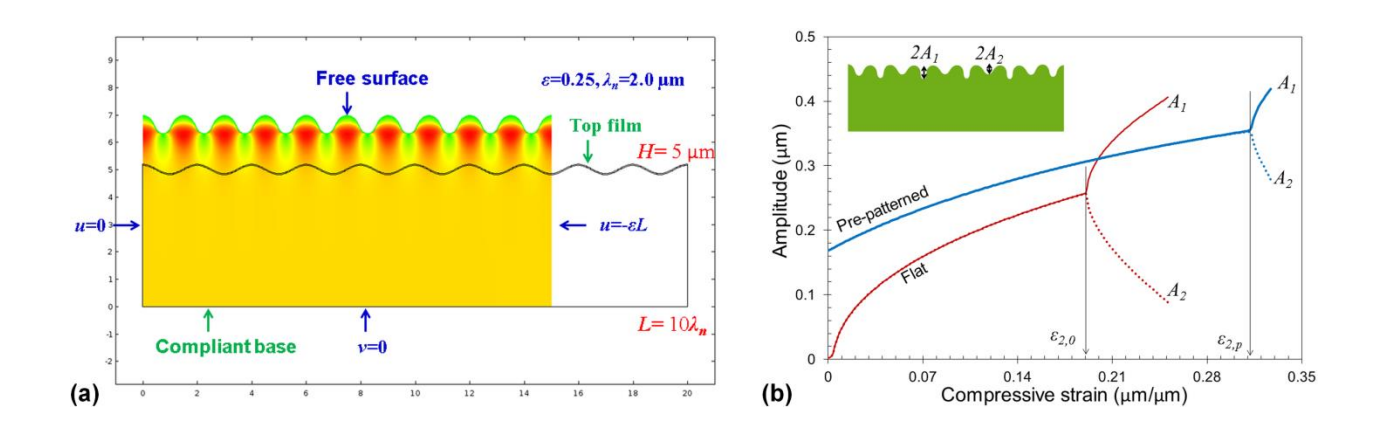


Fig. 4: (a) Finite element modeling of wrinkle formation during compression of a pre-patterned bilayer. Color information (green-to-red) represents increasing first principal strain in the system. (b) Growth in amplitude of wrinkles with increasing strain. The pre-pattern amplitude, natural period, thin film thickness, and Young's moduli ratio were [168 nm, 2.0 µm, 42 nm, 1690.4].

# 3 Characterization of onset strain tunability

To explain the effect of geometric pre-patterning on onset strain, one must first identify the cause of the period doubling phenomenon. Although small-strain linear elastic models can accurately predict the onset of sinusoidal wrinkles, they fail to predict onset of period doubling. Instead, one must account for the nonlinearity in the base at high strains to explain emergence of the period doubled mode.

# 3.1 Origin of tunability via geometric pre-patterning

Wrinkles are formed as a result of the competition between the deformation energy due to compression of base versus bending of top film. For linear materials, the energy of base  $(U_b)$  is directly related to the period of wrinkles and strain  $(U_b \sim \varepsilon \lambda)$ , whereas energy of the top film  $(U_t)$  is inversely related to the square of the period  $(U_t \sim \varepsilon/\lambda^2)$ . These scaling relationships are obtained from the linear-elastic deformation model as [11]:

$$U_{w} = \varepsilon \alpha \lambda + \varepsilon \frac{\beta}{\lambda^{2}}$$
 (2)

Here,  $U_w$  is the total strain energy of a flat bilayer system that undergoes wrinkling bifurcation  $(U_w = U_b + U_t)$ , the term with  $\alpha$  is the contribution due to the compression of the base and the term with  $\beta$  is the contribution due to the bending of the film. The parameters  $\alpha$  and  $\beta$  depend on the film thickness and material properties of the base and the film and are given by [11]:

$$\alpha = \frac{E_s}{3\pi} \tag{3}$$

$$\beta = \frac{\pi^2}{4} \frac{E_f h^3}{(1 - v^2_f)} \tag{4}$$

Here, h is the thickness of the top film,  $v_f$  is the Poisson's ratio of the top film,  $E_f$  and  $E_s$  are the Young's moduli, and the subscripts f and s refer to the top film and the base, respectively.

Equation 2 is valid for all wrinkle periods, i.e., it holds for both the natural and the period-doubled modes. For strain-controlled boundary condition, the natural period of the system can be obtained by minimizing the energy of the wrinkles with respect to the period; thus, the natural period  $(\lambda_n)$  is given by:

$$\lambda_n = \left(\frac{2\beta}{\alpha}\right)^{1/3} \tag{5}$$

For linear materials at low strains, this natural period is independent of the strain; thus, no period doubling would occur at high strains. In contrast, the deformation energy of the base for a nonlinear material, such as PDMS, is determined by a nonlinear coupling between the strain and the period. Due to this, the period corresponding to the minimum deformation energy state deviates away from the natural period with increasing strain. The onset strain for period doubling is the strain at which the  $2\lambda_n$  mode becomes energetically favorable over the  $\lambda_n$  mode.

Geometric pre-patterning delays the onset of period doubling by altering the nonlinear dependence of the base deformation energy on the period and amplitude of wrinkles. For a linear material, the ratio of deformation energy in the base for the  $2\lambda_n$  mode to that for the  $\lambda_n$  mode  $(U_{b,2\lambda}/U_{b,\lambda})$  is equal to 2 at all strains as predicted by Eq. 2. This ratio for a linear base remains unchanged for both the flat and the pre-patterned systems. However, the ratio  $U_{b,2\lambda}/U_{b,\lambda}$  drops with an increase in strain for a nonlinear base material such that the  $2\lambda_n$  mode becomes energetically favorable at high strains. The rate of decrease in the energy ratio with strain is lower for the case of a pre-patterned base. This manifests as an increase in the onset strain for the pre-patterned system.

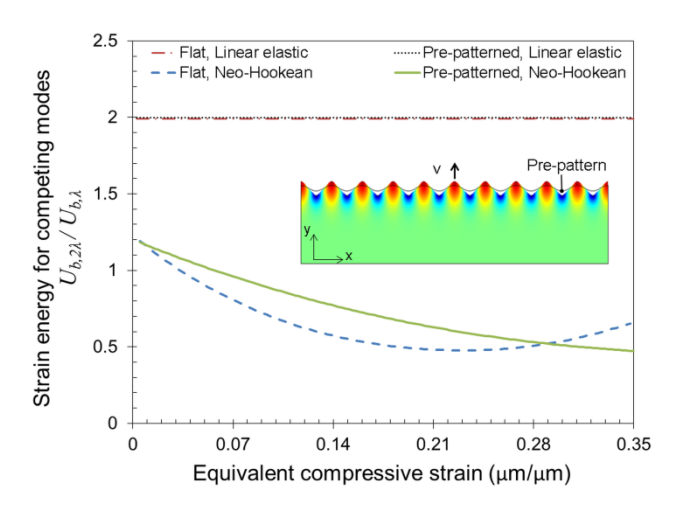


Fig. 5: Effect of strain on the ratio of the strain energy in the base for two competing wrinkle modes. The smaller period ( $\lambda$ ) was 2.25  $\mu$ m and the pre-pattern amplitudes were 0.084 times the periods.

To verify the effect of pre-patterning on onset strain, the deformation energy in a

nonlinear base material has been computationally evaluated. As illustrated in Fig. 5, the ratio of deformation energy  $(U_{b,2\lambda}/U_{b,\lambda})$  decreases at a slower rate for the pre-patterned bilayer as compared to the flat bilayer. Thus, the period doubling onset strain is higher for a pre-patterned bilayer. For these simulations, both linear elastic and nonlinear Neo-Hookean material models were used. To separately evaluate the energy in the base, a sinusoidal displacement  $(v = v_o \cdot \cos(2\pi X/\lambda))$  was applied to the top boundary of the base. This displacement is identical to the amplitude of the wrinkles; thus, the strain energy of this system is same as one would observe in the base of a bilayer undergoing wrinkling. This indirect evaluation technique for base energy has been extensively used in the literature to develop analytical models for bilayer wrinkling modes [11,12]. It has also been used during computational modeling of wrinkling to compare the effect of base nonlinearity on the wrinkling process [29]. Energy in the base was not evaluated via direct measurements of bilayer wrinkling systems because those measurements combine the contribution due to wrinkling and axial compression of the base. Thus, it is not possible to separately evaluate the base energy from post-buckling simulations of bilayer wrinkling.

To compare the results of this finite element simulation to that of bilayer wrinkling, one must link the applied displacement boundary condition to the equivalent strain for bilayer wrinkling. This is achieved by linking the displacement to the equivalent strain via kinematic relationships for bilayer wrinkling. For a flat bilayer, the amplitude of wrinkles (A) is kinematically related to the applied compressive strain  $(\varepsilon)$  and the period of wrinkles  $(\lambda)$  as:

$$\varepsilon = \left(\frac{\pi A}{\lambda}\right)^2 \tag{6}$$

For a pre-patterned bilayer, the amplitude of sinusoidal wrinkles is kinematically related to the strain as:

$$\varepsilon = \left(\frac{\pi A}{\lambda_p}\right)^2 - \left(\frac{\pi A_p}{\lambda_p}\right)^2 \tag{7}$$

Here,  $\lambda_p$  is the period of the pre-pattern and  $A_p$  is the amplitude of the pre-pattern, i.e., the amplitude at zero strain. These relationships are based on the approximation that there is negligible axial strain in the top film during wrinkle formation. This approximation is accurate for large Young's moduli ratio ( $E_f/E_s$ ). The second term on the left hand side of Eq. 7 is a non-

dimensional parameter  $(\varepsilon_p)$  that quantifies the size of the pre-pattern. The amplitude of the displacement that is applied at the top boundary of the base was evaluated as:  $v_o = A - A_p$ . Thus, for the simulations of Fig. 5, the equivalent strain was varied over a range and the corresponding amplitude of the applied displacement  $(v_o)$  was evaluated as:

$$v_{o} = \frac{\lambda_{p}}{\pi} \left( \varepsilon + \left( \frac{\pi A_{p}}{\lambda_{p}} \right)^{2} \right)^{0.5} - A_{p}$$
 (8)

These simulations (summarized in Fig. 5) demonstrate that the energy penalty for the period doubled mode increases when the base is pre-patterned, i.e., the ratio of energy of the  $2\lambda$  mode to that of the  $\lambda$  mode increases upon pre-patterning. Thus, pre-patterning the deformation energy delays the onset of period doubling.

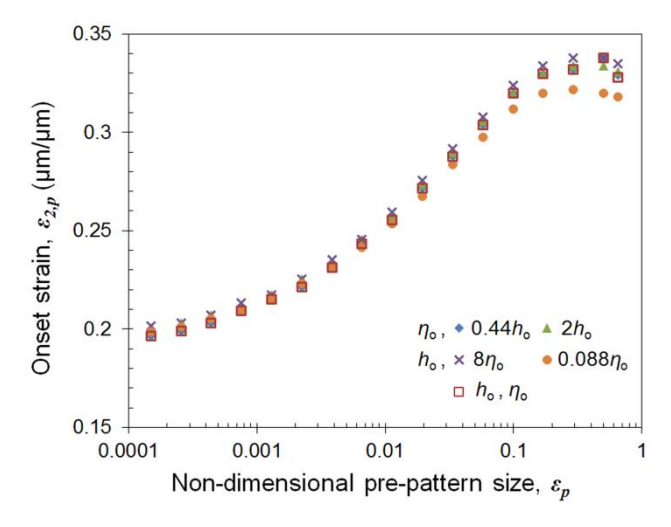


Fig. 6: Effect of pre-pattern size on the period doubling onset strain. Onset strain was evaluated for different natural periods by separately varying film thickness (h) and moduli ratio ( $\eta$ ). The natural periods were 1  $\mu$ m, 2.25  $\mu$ m, and 4.5  $\mu$ m. The parameter  $h_o$  was 47.5  $\mu$ m and  $\eta_o$  was 1690.4.

#### 3.2 Prediction of onset strain

As geometric pre-patterning affects the dependence of deformation energy on strain, it is expected that the onset strain can be tuned by varying the amplitude of the pre-pattern. This hypothesis was verified via finite element simulations of the bilayer wrinkling model. The results

for 85 separate pre-patterned bilayers are summarized in Fig. 6. It is observed that up to a limit, the onset strain increases with an increase in the size of the pre-pattern. Interestingly, for small to moderately large pre-patterns, this increase in onset strain is independent of the Young's moduli ratio and the film thickness. Instead, the onset strain depends only on the non-dimensional prepattern size  $(\varepsilon_p)$ . Thus, geometric pre-patterning is an elegant technique for suppression of period doubling; it can be successfully implemented even when one has limited knowledge about the material properties and/or thin film thickness - as is the case during wrinkle fabrication via plasma oxidation. It is important to note that despite its apparent universality, the relationship between onset strain and pre-pattern size is accurate only for those bilayer systems for which the Young's moduli ratio is sufficiently high (>100) and the period doubling mode is the preferred next higher order mode. This condition is satisfied by common engineered bilayer systems such as PDMS/glass and PDMS/metal bilayers but is not satisfied by biological bilayer systems with Young's moduli ratio of less than 10 wherein creases are the preferred next higher order mode [21, 30]. As engineered bilayer systems seldom have such low Young's moduli ratio, the prepatterning technique presented here is applicable for design and fabrication of a variety of functional wrinkled structures.

The non-dimensional pre-pattern size  $(\varepsilon_p)$  is obtained from the pre-pattern geometry as:

$$\varepsilon_{p} = \left(\frac{\pi A_{p}}{\lambda_{p}}\right)^{2} \tag{9}$$

Here,  $A_p$  is the pre-pattern amplitude and  $\lambda_p$  is the pre-pattern period that is equal to the natural period ( $\lambda_n$ ). Equation (9) is identical to the kinematic relationship that relates period, amplitude, and compressive strain during formation of wrinkles in flat bilayers. Thus, the non-dimensional pre-pattern size may be interpreted as the compressive strain that is required to generate the pre-pattern via wrinkling of an equivalent flat bilayer. The onset strain can be increased by a factor of 1.5 from ~20% to ~30% with a moderate pre-pattern size of 0.057. This corresponds to an aspect ratio  $(2A_p/\lambda_p)$  of 0.15, i.e., an amplitude of 150 nm for a period of 2  $\mu$ m. As this non-dimensional pre-pattern size ( $\varepsilon_p$ ) is significantly lower than the period doubling strain for flat bilayers, the pre-patterns can themselves be generated via wrinkling of flat bilayers.

The universality of the relationship linking the onset strain to the non-dimensional prepattern size  $(\varepsilon_p)$  at small to moderately large  $\varepsilon_p$  values can be explained in terms of another physical interpretation of  $\varepsilon_p$ . The non-dimensional pre-pattern size quantifies the "pre-strain" in the bilayer system because it represents the fractional increase in the curved length of the bilayer surface due to the pre-pattern (Eq. 7). This initial pre-strained state corresponds to a zero stress state, i.e., a state of zero deformation energy. As the subsequent single-period deformation mode is identical to the pre-patterned sinusoidal mode, this pre-strain quantitatively reduces the deformation energy but maintains the same qualitative deformation energy versus strain relationship. In addition, the period doubled mode emerges when the ratio of the base deformation energies in the natural and period doubled modes  $(U_{b,2\lambda}/U_{b,\lambda})$  drops below a fixed threshold value with increasing strain. For small to moderately large pre-strains, the combination of (i) same qualitative energy-strain relationship and (ii) ratio based threshold, suggests that the period doubling onset strain would be defined entirely by the pre-strain value  $(\varepsilon_p)$ . This expectation is supported by the results of computational modeling summarized in Fig. 6. For large pre-strains (i.e.,  $\varepsilon_p > 0.1$ ), this expectation of universality is not valid anymore; instead, the period doubling onset strain varies with the material properties and film thickness.

For large pre-patterns, the period doubling onset strain approaches an optimum value and then starts decreasing with further increase in the pre-pattern size. This observation is consistent with the deformation energy versus equivalent strain behavior of the base that is shown in Fig. 5. At very large strains, the ratio of  $U_{b,2\lambda}/U_{b,\lambda}$  for flat bilayers exceeds the ratio for pre-patterned bilayers. Thus, for large pre-patterns, the  $2\lambda_n$  mode becomes energetically more favorable in the pre-patterned bilayers than in the flat bilayers. This reversal of energy versus pre-pattern size trend then manifests as a reversal in the period doubling suppression behavior of pre-patterns above pre-pattern sizes ( $\varepsilon_p$ ) of ~ 0.1. Nevertheless, the onset strain can be deterministically tuned via geometric pre-patterning in the range of ~20% to ~30% strain before this reversal limit is encountered.

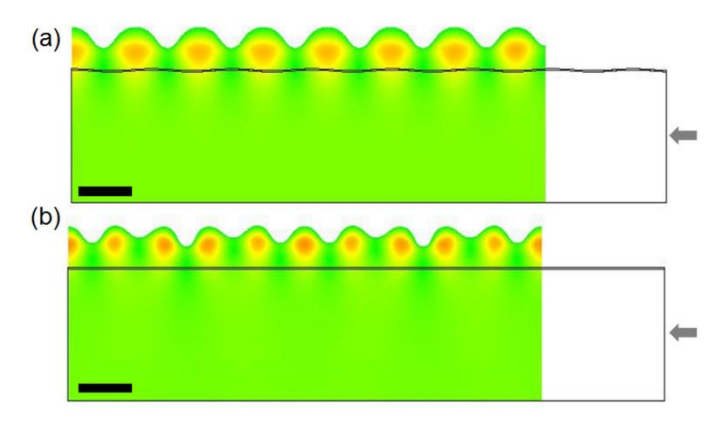


Fig. 7: Finite element model of (a) flat and (b) pre-patterned bilayers for the case when the pre-pattern and natural periods are not identical. The natural period of the bilayers was 2.25  $\mu$ m and the pre-pattern period and amplitude were 3  $\mu$ m and 36 nm. The onset strain for flat bilayer is 0.19 whereas the onset strain for the pre-patterned bilayer is 0.225. The strain in the two bilayers is 0.205. Color information (green-to-red) represents increasing first principal strain in the system. Scale bars are 2  $\mu$ m long.

### 4 Limitations of pre-patterning technique

#### 4.1 Limitations of fabrication technique

Despite its elegance, the need for the pre-pattern period to be 'identical' to the natural period may be perceived as a limitation for practical implementation of this technique. When the pre-pattern period is not identical to the natural period, a multi-period hierarchical pattern is expected [10]. However, this concern can be overcome by the mode lock-in phenomenon that occurs during compression of pre-patterned bilayers [31]. We have recently identified that the emergence of the hierarchical mode is preceded by a mode locked state wherein the pre-pattern mode persists [25,31]. When the pre-pattern period is 'substantially similar' to the natural period, it is possible for the single-period mode to persist beyond the period doubling onset strain as illustrated in Fig. 7. The next step to developing this technique would be to quantify this substantial similarity regime. Nevertheless, it is evident from the experiments performed here that this limit is higher than the variations in  $\lambda_p/\lambda_n$  that arise due to fabrication errors; therefore, this scheme can be successfully implemented even with an imperfect match between the prepattern and natural periods.

# 4.2 Limitations of computational modeling

Although a base pre-stretching based technique has been used herein to generate film compressive strains during physical experiments, finite element modeling has been performed by simultaneously compressing the film and the base without any base pre-stretch. This is because of the inability to accurately implement a base pre-stretch based computational technique in the COMSOL software package that was used here. For wrinkling computations using other packages, the standard technique for implementing pre-stretch involves first stretching the bilayer and then setting the stress in the top layer to zero. This condition then mimics the physical experiments wherein an unstressed thin film is deposited on top of a pre-stretched base layer. When implemented in COMSOL, this technique leads to an inaccurate nonlinear straindisplacement relationship for the thin film as the strain is evaluated using the shorter initial unstretched configuration of the top film instead of the unstressed length of the film on a stretched base. In the absence of an accurate pre-stretching technique, a direct film compression technique has been used here. As the pre-stretch in the base affects the period doubling onset strain [22-24], this approximation somewhat limits the quantitative applicability of the technique presented here. Specifically, the onset strain due to pre-patterning may not be identical to those in Fig. 6 when this pre-patterning based technique is physically implemented in pre-stretched bilayer systems. Nevertheless, the following observations are still applicable: (i) pre-patterns delay the onset of period doubling as verified by physical experiments performed here and (ii) universality of the onset strain versus pre-pattern size at small to moderately large pre-pattern sizes. Thus, when the pre-stretch is non-zero but held constant, one may still apply the results from Fig. 6 with the modification that the onset strain for flat pre-stretched bilayer is higher than the flat unstretched bilayer. To do so, one may experimentally observe the period-doubling onset strain in a flat bilayer at the applied pre-stretch and then use it as an offset to increase the values predicted by the curve of Fig. 6 to predict the effect of pre-patterning. For typical pre-stretch values of ~20%, such an approach is expected to require an increase of ~ 6% strain [23] over the values for the onset strain obtained from Fig. 6 to generate realistic predictions of the onset strain in prestretched and pre-patterned bilayers.

#### 5 Conclusions

In summary, a practical technique for delaying the onset of period doubling via geometric pre-patterning has been demonstrated here. The onset strain for period doubling can be increased from a typical value of 20% to >30% strain with a moderate pre-pattern aspect ratio of 0.15. For small to moderately large pre-patterns, the suppression behavior is fully captured by the pre-pattern geometry. Thus, this technique can be implemented even with limited knowledge about the properties of the wrinkling bilayer system. Pre-patterning with the natural period of the system maintains the single-period morphology of the wrinkles at high strains. Consequently, the operating range of a variety of stretch-tunable functional devices can be increased by at least 50% simply by replicating the wrinkled patterns and repeating the wrinkle fabrication steps on the pre-patterned system.

#### References

- [1] Ahmed, S. F., Rho, G.-H., Lee, K.-R., Vaziri, A., and Moon, M.-W., 2010, "High aspect ratio wrinkles on a soft polymer," Soft Matter, 6(22), pp. 5709-5714.
- [2] Bowden, N., Brittain, S., Evans, A. G., Hutchinson, J. W., and Whitesides, G. M., 1998, "Spontaneous formation of ordered structures in thin films of metals supported on an elastomeric polymer," Nature, 393(6681), pp. 146-149.
- [3] Chen, X., and Yin, J., 2010, "Buckling patterns of thin films on curved compliant substrates with applications to morphogenesis and three-dimensional micro-fabrication," Soft Matter, 6(22), pp. 5667-5680.
- [4] Genzer, J., and Groenewold, J., 2006, "Soft matter with hard skin: From skin wrinkles to templating and material characterization," Soft Matter, 2(4), pp. 310-323.
- [5] Kim, J. B., Kim, P., Pegard, N. C., Oh, S. J., Kagan, C. R., Fleischer, J. W., Stone, H. A., and Loo, Y.-L., 2012, "Wrinkles and deep folds as photonic structures in photovoltaics," Nat Photonics, 6(5), pp. 327-332.
- [6] Lin, P. C., and Yang, S., 2007, "Spontaneous formation of one-dimensional ripples in transit to highly ordered two-dimensional herringbone structures through sequential and unequal biaxial mechanical stretching," Appl. Phys. Lett., 90(24), p. 241903.
- [7] Mei, Y., Kiravittaya, S., Harazim, S., and Schmidt, O. G., 2010, "Principles and applications of micro

- and nanoscale wrinkles," Materials Science and Engineering: R: Reports, 70(3-6), pp. 209-224.
- [8] Watanabe, M., and Mizukami, K., 2012, "Well-Ordered Wrinkling Patterns on Chemically Oxidized Poly(dimethylsiloxane) Surfaces," Macromolecules, 45(17), pp. 7128-7134.
- [9] Ohzono, T., and Monobe, H., 2012, "Microwrinkles: Shape-tunability and applications," J. Colloid Interface Sci., 368(1), pp. 1-8.
- [10] Chiche, A., Stafford, C. M., and Cabral, J. T., 2008, "Complex micropatterning of periodic structures on elastomeric surfaces," Soft Matter, 4(12), pp. 2360-2364.
- [11] Groenewold, J., 2001, "Wrinkling of plates coupled with soft elastic media," Physica A: Statistical Mechanics and its Applications, 298(1-2), pp. 32-45.
- [12] Jiang, H., Khang, D.-Y., Song, J., Sun, Y., Huang, Y., and Rogers, J. A., 2007, "Finite deformation mechanics in buckled thin films on compliant supports," Proceedings of the National Academy of Sciences, 104(40), pp. 15607-15612.
- [13] Saha, S. K., and Culpepper, M. L., 2015, "Design of a Compact Biaxial Tensile Stage for Fabrication and Tuning of Complex Micro- and Nano-scale Wrinkle Patterns," ASME Journal of Micro and Nano-Manufacturing, 3(4), pp. 041004-041004.
- [14] Huh, D., Mills, K. L., Zhu, X., Burns, M. A., Thouless, M. D., and Takayama, S., 2007, "Tuneable elastomeric nanochannels for nanofluidic manipulation," Nat Mater, 6(6), pp. 424-428.
- [15] Chung, S., Lee, J. H., Moon, M.-W., Han, J., and Kamm, R. D., 2008, "Non-Lithographic Wrinkle Nanochannels for Protein Preconcentration," Adv. Mater., 20(16), pp. 3011-3016.
- [16] Harrison, C., Stafford, C. M., Zhang, W., and Karim, A., 2004, "Sinusoidal phase grating created by a tunably buckled surface," Appl. Phys. Lett., 85(18), pp. 4016-4018.
- [17] Yu, C., O'Brien, K., Zhang, Y.-H., Yu, H., and Jiang, H., 2010, "Tunable optical gratings based on buckled nanoscale thin films on transparent elastomeric substrates," Appl. Phys. Lett., 96(4), p. 041111.
- [18] Da, Y., Jing, F., Rui, M., Xu-Lin, Z., Yue-Feng, L., Tong, Y., and Hong-Bo, S., 2015, "Stability Improved Stretchable Metallic Gratings With Tunable Grating Period in Submicron Scale," Journal of Lightwave Technology, 33(15), pp. 3327-3331.
- [19] Brau, F., Vandeparre, H., Sabbah, A., Poulard, C., Boudaoud, A., and Damman, P., 2011, "Multiple-length-scale elastic instability mimics parametric resonance of nonlinear oscillators," Nat Phys, 7(1), pp. 56-60.
- [20] Zhao, Y., Cao, Y., Hong, W., Wadee, M. K., and Feng, X.-Q., 2015, "Towards a quantitative understanding of period-doubling wrinkling patterns occurring in film/substrate bilayer systems,"

- Proceedings of the Royal Society of London A: Mathematical, Physical and Engineering Sciences, 471(2173).
- [21] Budday, S., Kuhl, E., and Hutchinson, J. W., 2015, "Period-doubling and period-tripling in growing bilayered systems," Philosophical Magazine, 95(28-30), pp. 3208-3224.
- [22] Cao, Y., and Hutchinson, J. W., 2012, "Wrinkling Phenomena in Neo-Hookean Film/Substrate Bilayers," ASME Journal of Applied Mechanics, 79(3), pp. 031019-031019.
- [23] Auguste, A., Jin, L., Suo, Z., and Hayward, R. C., 2014, "The role of substrate pre-stretch in post-wrinkling bifurcations," Soft Matter, 10(34), pp. 6520-6529.
- [24] Chen, Y.-C., and Crosby, A. J., 2014, "High Aspect Ratio Wrinkles via Substrate Prestretch," Adv. Mater., 26(32), pp. 5626-5631.
- [25] Saha, S. K., and Culpepper, M. L., 2016, "Deterministic Switching of Hierarchy during Wrinkling in Quasi-planar Bilayers," Adv. Eng. Mater., 18(6), pp. 938-943.
- [26] Bowden, N., Huck, W. T. S., Paul, K. E., and Whitesides, G. M., 1999, "The controlled formation of ordered, sinusoidal structures by plasma oxidation of an elastomeric polymer," Appl. Phys. Lett., 75(17), pp. 2557-2559.
- [27] Saha, S. K., 2014, "Predictive Design and Fabrication of Complex Micro and Nano Patterns via Wrinkling for Scalable and Affordable Manufacturing," Doctor of Philosophy thesis, Massachusetts Institute of Technology, Cambridge, MA. <a href="http://hdl.handle.net/1721.1/93860">http://hdl.handle.net/1721.1/93860</a>
- [28] Saha, S.K., and Culpepper, M.L., 2016, "Method to Fabricate Pre-Patterned Surfaces during Manufacture of Complex Wrinkled Structures" U.S. Patent Application Publication No. US20160039142.
- [29] Hutchinson, J. W., 2013, "The role of nonlinear substrate elasticity in the wrinkling of thin films," Philosophical Transactions of the Royal Society A: Mathematical, Physical and Engineering Sciences, 371(1993).
- [30] Wang, Q., and Zhao, X., 2014, "Phase diagrams of instabilities in compressed film-substrate systems," ASME Journal of Applied Mechanics, 81(5), p. 051004.
- [31] Saha, S.K., 2017, "Sensitivity of the mode locking phenomenon to geometric imperfections during wrinkling of supported thin films", International Journal of Solids and Structures, 109, pp. 166–179.